Simulation of the Performance of Kevlar Impregnated Shear Thickening Fluid Ballistic Test Results

Ridwan Prasetya[1], Andoko[1*], Suprayitno[1], Retno Wulandari[1], Prihanto Trihutomo[1], Kenji Mishima[2], Dawid Janas[3]

[1]*Department of Mechanical and Industrial Engineering, Engineering Faculty, Universitas Negeri Malang, Semarang Street 5, Malang City, 65145, Indonesia*
[2]*Department of Chemical Engineering, Faculty of Engineering, Fukuoka University, Fukuoka City, 814-0180, Japan*
[3]*Department of Organic Chemistry, Biochemistry, and Biotechnology, Faculty of Chemistry, Silesian University of Technology, Krzywoustego 8, 44-100 Gliwice, Poland*
**Corresponding author: andoko.ft@um.ac.id*

Article history:
Received: 23 December 2023 / Received in revised form: 14 March 2024 / Accepted: 27 April 2024
Available online 23 May 2024

ABSTRACT

This study explores the enhancement of Kevlar fabric's ballistic performance through impregnation with Shear Thickening Fluid (STF) for potential application in soft body armor. The experimental approach often fails to elucidate mechanical phenomena critical for the development of lightweight and high-strength body armor designs. To address this limitation, the finite element method, specifically using ANSYS/LS-DYNA R.13, was employed for a comprehensive analysis. The simulation aimed to evaluate the impact of STF on Kevlar fabric by assessing projectile velocity, force exerted by the projectile onto the fabric, displacement, stress distribution, and fabric failure mechanisms. Kevlar yarn was modeled as a shell element formed into fabric with a sine wave profile, investigating two types of STF: SiO_2-PEG200 (S0) and SiO_2-PEG200-B_4C (S1), differing in maximum viscosities. The addition of STF resulted in increased coefficients of friction on Kevlar, with the highest values observed for the SiO_2-PEG200-B_4C impregnated fabric (μ_{s1} =0.87 and μ_{d1}=0.82). The incorporation of the second STF type (S1) significantly reduced the projectile's velocity from an initial 200 m/s to 153.2 m/s upon impact. Additionally, the force on the S1 fabric surged to 121,556 N, a threefold increase compared to neat Kevlar. STF's influence was further evidenced by enhanced fabric displacement and more uniform stress distribution upon ballistic impact. The fabric's thickening upon failure indicated STF's ability to enlarge the deformation area, facilitating uniform distribution of ballistic kinetic energy across the impact zone. Notably, the fabric impregnated with the second type of STF, featuring boron carbide (S1), demonstrated superior ballistic performance. This study concludes that STF-impregnated Kevlar fabric, particularly the SiO_2-PEG200-B_4C variant, not only surpasses the ballistic performance of neat Kevlar but also meets the criteria for NIJ Level IIIA standards, highlighting its potential as a highly effective material for advanced soft body armor designs.

Keywords: *Ballistics, performance, Kevlar, simulation, STF*

I. Introduction

Soft body armor is part of an army protection device that requires high strength, flexibility, lightweight, and resistance to ballistic penetration or sharp objects [1]. Soft body armor is made of high-strength flexible fabrics such as Kevlar, Twaron, aramid, Spectra, Dyneema, etc [2]. Kevlar is a type of fabric widely used because of its resistance to puncture and abrasion [3]. In body armor, Kevlar is generally arranged in as many as 20 to 50 layers [4]. This large number of layers leads to an increase in armor weight, which also reduces

DOI: 10.17977/um016v8i12024p054

flexibility and mobility. In addition, Kevlar has the disadvantage that it is easily torn due to friction and high pressure. One way to improve Kevlar performance is to impregnate it with Shear Thickening Fluid (STF) [5]. STF is a non-Newtonian fluid whose viscosity increases when passing through the critical shear rate [6]. STF is generally made of solid particles (silica) and dispersing liquid (polyethylene glycol) [7]. The latest development, STF, is enhanced with additives to improve its thickening properties, which have an impact on increasing energy absorption [8]. Wagner et al. [9] first combined STF in Kevlar and, through experimental research, stated that ballistic performance on Kevlar increased. Furthermore, other researchers carried out developments that showed similar results, namely, the addition of STF can improve ballistic performance in Kevlar [3], [10]–[12]. In addition, increasing the nature of energy absorption by engineering STF rheology also develops, namely by adding additive materials. Additives contribute to blocking fluid flow during increased shear stress, which in turn improves the viscosity profile at STF [5]. The combination of soft body armor fabric with STF and additive materials leads to positive results in absorption of kinetic energy from ballistics and reduced deformation.

Research on the performance of Kevlar impregnated with STF due to ballistics is important to develop effective and efficient body protective materials. One of the performance evaluations of Kevlar is post-firing failure analysis. Understanding the failure mechanism and its types is an approach used in protective systems that is critical to increasing their resistance to ballistics. Through failure studies on soft body armor, researchers can develop new armor by improving performance and protection capacity [13], [14]. The failure mechanism can be approached through experimentation and numerical simulation. Experimental research has been conducted to detect impact failure in armor fabrics on different size scales, including the number of shots, number of layers, fabric, and fibers [15]. The experimental results revealed that the durability of impact on armor is influenced by various factors such as fabric material properties, fabric patterns, and stress states [15]. Computer modeling is also used to understand the complexity of penetration and perforation during impact. Simulation helps describe how material flows, faults, and failures occur and can provide insight into critical conditions for impact failure. The simulated approach provides several advantages over experimental methods, including providing an understanding of the protective fabric behavior under various conditions, being able to decipher complexity during ballistic impacts with varying variations in the impact zone, enabling parametric analysis of material properties that contribute to future material development, and being able to provide quantitatively accurate predictions of penetration events [16], [17]. In addition, the simulated approach can make up for the shortcomings of the experimental method, namely the analysis of mechanical details during the ballistic process [18],[19].

The study of failure in STF-impregnated soft body armor is interesting because it can help optimize durability and reduce weight from protective systems [20]. STF added to the fabric is realized in an increase in the coefficient of friction between yarns. Previous research by and [21] indicates that increased friction may increase the load-bearing area on the fabric. This mechanism is further described by [18] which states that increased friction can increase the bearing area of the fabric and the tension in the deformed area more uniformly. Based on previous research, increased friction can improve ballistic performance in Kevlar but the specific mechanism of this phenomenon is not yet clear. In this study, a simulation of the performance of STF-impregnated Kevlar due to ballistics will be carried out. STF added to kevlar consists of 2 types, namely those composed of SiO_2-PEG200 and SiO_2-PEG200-B_4C. Boron carbide is an additive material because it can increase the thickening profile of STF, lightweight, hard, and high strength, so it has the potential to become body armor. Kevlar performance is evaluated through projectile velocity. This research is also relevant to the current context, where security threats and armed conflicts are still common in various parts of the world. In addition, this research can contribute to the development of science and technology, especially in the field of defense and security. So, the aim of this research is to analyze the performance of Shear Thickening Fluid (STF)-impregnated Kevlar due to ballistics through the evaluation of projectile velocity, projectile-to-fabric force, displacement, stress, and fabric failure mechanisms.

II. Materials and Methods

1. Materials

Materials for projectiles and fabrics are shown in Table 1. Projectiles are modeled as elastic components (*MAT_ELASTIC) because damage and deformation during ballistic processes are negligible, so projectiles are considered linear materials. Kevlar fabric is made of yarn fibers where the modulus of elasticity and strength depends on the direction of the fiber. In this case, the material for the fabric is modeled as an orthotropic constitutive model (*MAT_ORTHOTROPIC_ELASTIC). The failure criterion for thread is a tensile failure criterion, which is that the thread will break when the applied stress reaches the limit of the tensile strength of the material [10]. This criterion is inputted as the keyword MAT_ADD_EROSION with the limit of tensile strength of Kevlar fabric as 2 GPa.

Table 1. Projectile and Kevlar materials [16]

Materials	Keywords	Parameters		
Projectile	MAT_ELASTIC	RO (tonne/mm^3)	E (MPa)	PR
		7.85E-09	1.9E+5	0.305
Kevlar	ORTHOTROPIC_ ELASTIC		RO (tonne/mm^3)	
			1.44E-09	
		EA (MPa)	EB (MPa)	EC (MPa)
		5.57E+4	2000	2000
		GAB (MPa)	GBC (MPa)	GCA (MPa)
		2000	2000	2000

RO : Density; E : Modulus Young; PR : Poisson Ratio; EA : Modulus Young in x direction; EB : Modulus Young in y direction; EC : Modulus Young in z direction; GAB : Shear Modulus in xy; GBC : Shear Modulus in yz; GCA : Shear Modulus in xz.

2. Methods

The method used in this research is computational. Computational modeling on STF-impregnated Kevlar is carried out using ANSYS/LS-DYNA R.13 software, which is completed with 3 steps, namely pre-processing, processing, and post-processing. The diagram for these stages is shown in Figure 1.

Projectile and Kevlar geometry: A spherical projectile with a diameter of 6 mm modeled as a solid. Kevlar fabrics are modeled as yarns at the finite element-based membrane level simulated using LS-DYNA. The cross-section of a single thread can be modeled in elliptical and wavy shapes following the sine function. The specific equation for expressing the form and function of the fabric is expressed by equations (1) and (2) with the visualization in Figure 2 [18].

Vol. 8, No. 1, July 2024, pp. 54-70

$$\frac{x^2}{a} + \frac{y^2}{b} = 1 \quad \text{(1)}$$

$$y = A \sin\left(\frac{2\pi}{T} x\right) \quad \text{(2)}$$

where:
a : elliptical major axis (mm)
b : Minor axis of ellipse (mm)
A : Sine function amplitude(mm)
T : fabric length in one cycle (mm)

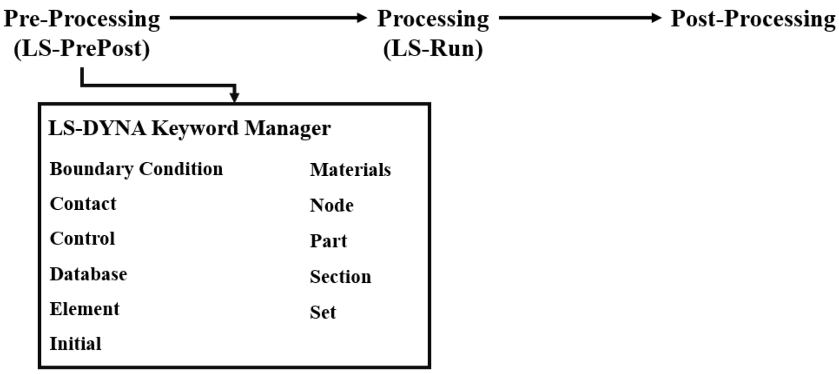

Fig. 1. Simulation steps

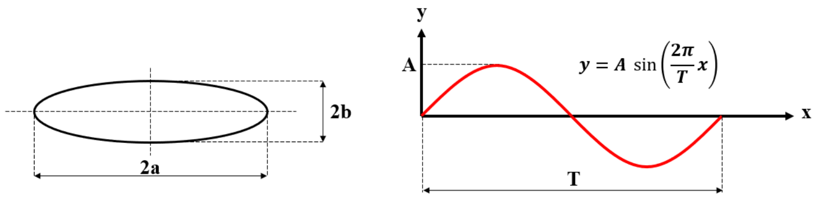

Fig. 2. Cross-sectional shape and fabric profile

The above parameter values for Kevlar are based on [16], as shown in Table 2.

Table 2. Kevlar fabric dimensions

Parameter (mm)	Warp	Weft
2a	0.585	0.655
2b	0.089	0.085
A	0.097	0.122
T	2.982	2.997

Projectiles and yarns arranged into fabric are modeled in 1/4 section to reduce computational time, as shown in Figure 3. The dimensions of the fabric in the simulation are 50 x 50 mm. Projectiles modeled as solid shapes produce element counts of 10206 and nodes of 11314, while fabrics modeled as shell elements produce 11850 elements and 18088 nodes.

Boundary conditions: The boundary conditions on the fabric are shown in Figure 4, where there are 2 sides as fixed support and 2 sides as symmetry. In fixed support, the degrees of freedom of all nodes are held (111111). Two symmetry planes, namely the X and

Z planes, are used. The degrees of freedom for X plane are (100011) and Z (001110). This limit condition uses the keyword BOUNDARY_SPC_SET. The contact during the simulation process consists of contact between fabrics (warp and weft) and fabric with projectiles. Fabric contact is modeled as an interface with the keyword AUTOMATIC_SURFACE_TO_SURFACE. The value of the coefficient of friction for neat Kevlar is 0.22. On the contact between the projectile and the fabric, the keyword ERODING_SURFACE_TO_SURFACE was chosen because the fabric failed during contact with the projectile. The initial velocity is applied to the projectile in the y direction with the keyword INITIAL_VELOCITY_GENERATION.

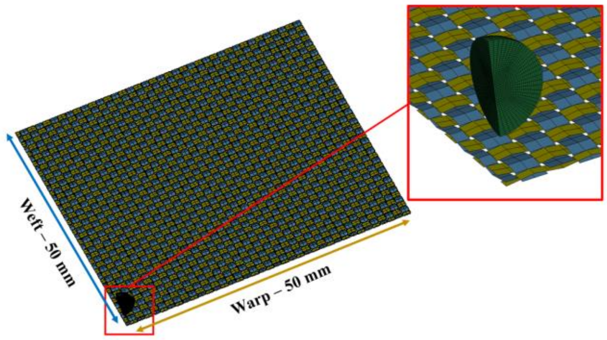

Fig. 3. Fabric and projectile models

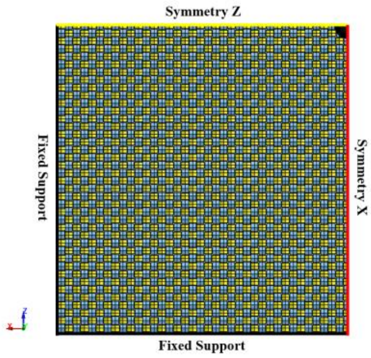

Fig. 4. Fabric Boundary Conditions

Model Validation: Impact simulation models on ballistics need to be validated to ensure that the models built are the same and accurately describe the actual model [22]. Validation of simulation models is carried out by creating a model with the same data input and results as the ballistic test results.

Implementation of STF's effect on Kevlar: The experimental design for this research is to focus on the performance of Kevlar fabric reinforced with STF and without STF (shown in Table 3 for Kevlar with STF (S0 and S1) and without STF (Kevlar)). The presence of STF in Kevlar fabric influences the form of increased friction between yarns during impact. Previous research, both experimentally and computationally, showed that the increased friction between fabrics caused by STF impregnation is an increase in ballistic performance in fabrics [21], [23], [24]. Therefore, implementing the STF effect on Kevlar is to increase the coefficient of friction between yarns. The coefficient of friction between yarns on Kevlar fabrics is reported by [11] be $\mu_s = 0.22$ and $\mu_d = 0.20$. This value needs to be modified to give STF an effect on Kevlar so that the computational analysis is the same as the experiment. The value of the friction coefficient between fabrics given STF was determined through trial & error in ballistic simulations whose results were compared with experimental. Experimental data of ballistic test results on Kevlar impregnated by STF are shown in Table 3. Shear Thickening Fluid used consists of 2 types, namely without and with the addition of additive materials. STF without additives consists of SiO_2 (25 wt%) and PEG200 (75 wt%). While the additives used are B_4C mixed with a concentration of 7.5 wt% in SiO_2 (25 wt%) and PEG200 (67.5 wt%). The maximum viscosity at STF is obtained using a rheometer at a shear rate of 0-1000/s. Initial and final velocity data were obtained through ballistic tests using an air gun. The air gun used is the PCP Ghost Warrior, which has a tube volume of 360 cc and a pressure of 3000 psi, which can fire bullets at speeds of up to 350 m/s. The bullet used is a steel ball with a diameter of 6 mm with a mass of 0.7 grams. Thus, the soft body armor developed is included in the NIJ level IIIA standard. The initial and final velocity of the projectile was measured using velocimetry installed before and after the sample. STF, with the addition of additives, increases its maximum viscosity value, which has an impact on better absorption of ballistic energy.

Table 3. Experimental ballistics test results

Code	Composite Composition	STF Maximum Viscosity (Pa.s)	Initial Velocity (m/s)	Final Velocity (m/s)
Kevlar	Kevlar	-	255.2 257 258	234 240 227
S0	Kevlar + STF (SiO_2 25 wt%+PEG200 75 wt%)	511.46	252.2 246.5 240.8	226 222 209
S1	Kevlar + STF (SiO_2 25 wt%+B_4C 7.5 wt%+PEG200 65 wt%)	1063.8	265 262 261	220 215 214

III. Results and Discussions

1. Model Validation

The simulation results on pure Kevlar fabrics impacted by ballistics are shown in Figure 5 and numerically in Table 4.

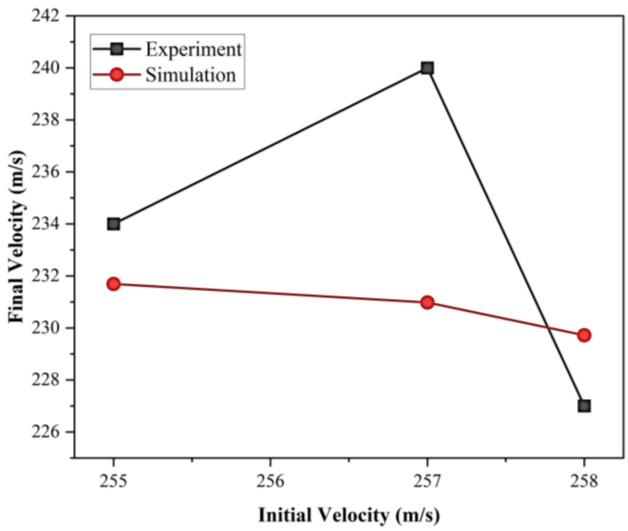

Fig. 5. Validate simulation results with experiments

The simulation results are compared with the experimental as validation of the built model. The initial velocity at which the experimental results are duplicated in modeling. The average velocity of the projectile after passing through the fabric in the experimental results was 233.7 m/s, and in the simulation, 230.8 m/s. The difference between the two is 2.9 m/s, or an error of 1.23%. The error value is below 5%, which indicates that the simulation results are acceptable/ in accordance with the experimental results [25].

2. Coefficient of Friction

The coefficient of friction between yarns is determined through trial & error on ballistic simulations whose results are compared with experimental. It can be seen in Table 4, simulation results for S0 and S1. The results of S0 and S1 refer to the results of experiments to determine the value of the coefficient of friction in fabrics due to the influence of STF. The value of the coefficient of friction in Kevlar added by STF has increased compared to neat Kevlar. STF has an influence on Kevlar in the form of increasing the frictional force of the yarn interface. This is in accordance with the results of the study $\mu_{s_1} = 0.55, \mu_{d_1} = 0.41, \mu_{s_2} = 0.87 \mu_{d_2} = 0.82$ [7], [11], [26]. The coefficient of friction in S1 is greater than that of S0; this is related to the maximum viscosity value in S1 STF liquid, which is greater than S0. STF forms a thin layer on the surface of the thread [27]. Higher viscosity values will result in thicker layers and increase the coefficient of friction between yarns.

Table 4. Results of simulations and experiments

Target Type	Initial Velocity (m/s)	Final Velocity (m/s)		Residual Velocity (m/s)		Error (%)
		Exp.	Sim.	Exp.	Sim.	
Kevlar	255.2	234	231.69	21.2	23.31	3.76
	257.0	240	230.89	17.0	26.11	0.99
	258.0	227	229.72	31.0	28.28	1.20
S0	240.8	209	210.60	31.8	30.20	0.77
	246.5	222	213.20	33.3	33.30	3.96
	252.2	226	223.50	26.2	28.70	1.11
S0	261.0	214	219.18	47.0	41.82	2.42
	262.0	215	231.26	47.0	30.74	2.91
	265.0	220	226.96	45.0	38.04	3.16

3. Projectile Velocity

The velocity profile of the projectile before and after firing the Kevlar is shown in Figure 6. The initial velocity of the projectile passing through the three fabric variations is the same at 200 m/s. In neat Kevlar, the velocity of the projectile drops to 193.76 m/s at 7.65 x 10^{-5} s and then tends to be constant to 0.00025 s. Kevlar impregnated by the first type of STF (S0) experienced a lower decrease in projectile velocity than neat Kevlar, up to 1.64x10^{-4} s at 168.15 m/s. The highest decrease in projectile velocity was when passing through Kevlar to which the second type of STF (S1) was added. The descent time is longer at 1.76x10^{-4} s at 153.22 m/s. Based on the results of the projectile velocity during passing through the fabric, the addition of STF to the Kevlar can effectively absorb the velocity of the projectile indicated by the reduced velocity of the projectile after passing through the fabric.

4. Projectile Impact Force

The impact force of the projectile on the fabric is the force generated by the projectile when it hits the fabric. The impact force of the projectile for each fabric is shown in Figure 7. In neat Kevlar, the impact force by the projectile is highest at 35845 N. Kevlar, which STF added, experienced an increase in projectile impact force with a value of 110,541 and 121,556 N for S0 and S1. STF-impregnated fabric increases projectile impact force by up to 3 times. The impact force from the projectile to the fabric can be used to find out how much penetration the projectile has into the fabric. The magnitude of the impact force of the projectile is proportional to the resistance of the fabric to impact loads.

Vol. 8, No. 1, July 2024, pp. 54-70

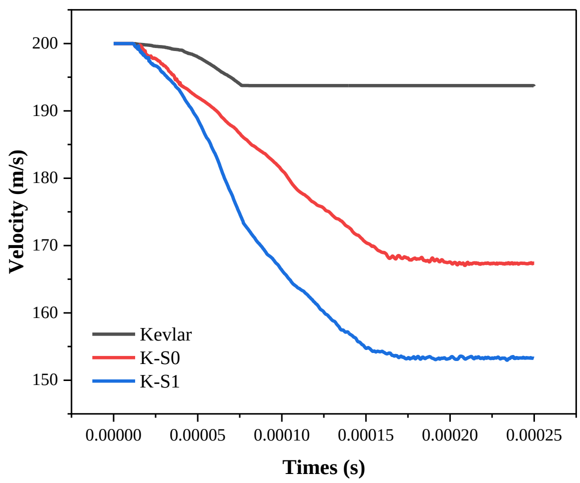

Fig. 6. Projectile velocity profile

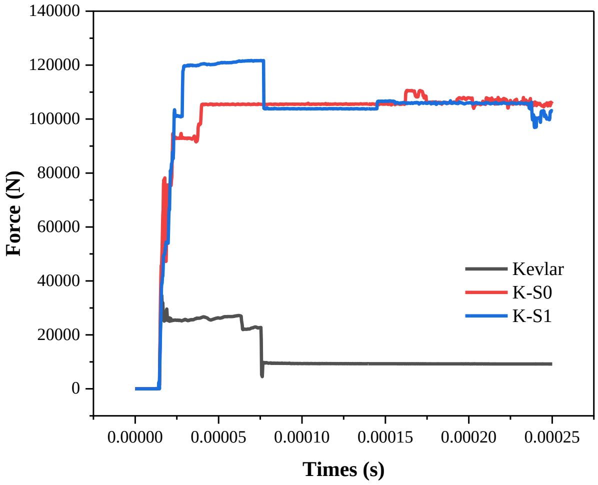

Fig. 7. Impact force by projectile to fabric

5. *Deformation*

Figure 8 shows the displacement in the fabric (8a) and projectile (8b) during the impact process visualized in Figure 9(a)-(e).

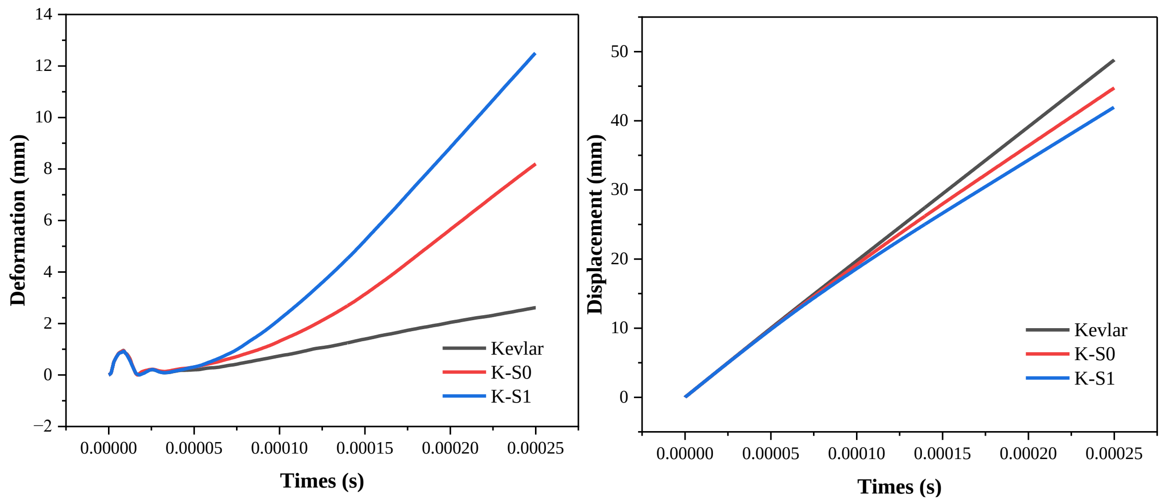

(a) (b)

Fig. 8. (a) Fabric deformation; (b) Projectile displacement

The largest fabric displacement occurs in Kevlar added with STF, which has the highest viscosity (S1) of 12.5 mm, followed by S0 (8.2 mm), and finally, neat Kevlar of 2.6 mm. The displacement condition of the projectile is inversely proportional to the displacement of the fabric. Projectiles hitting neat Kevlar traveled farther (48.72 mm) than those hitting S0 (44.7 mm) and S1 (41.9 mm). The two states between the displacement of the fabric and the projectile give the relationship that the greater the displacement of the fabric, the smaller the displacement of the projectile, which indicates that the fabric provides resistance to the projectile by deforming greater [15], [16].

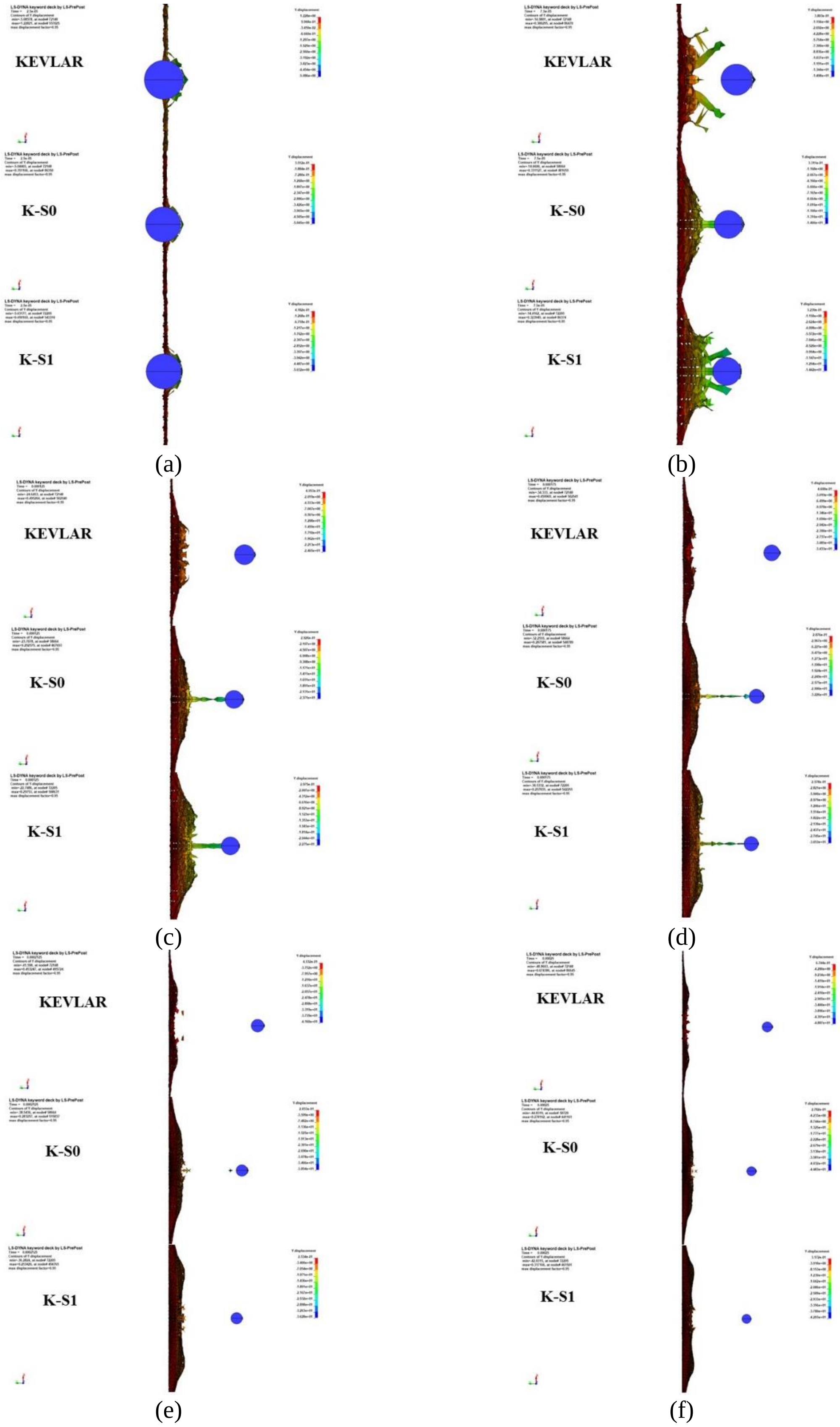

Fig. 9. Deformation of fabrics and projectiles at time (a) 0.000025; (b) 0.000075; (c) 0.000125; (d) 0.000175 (e) 0.0002125 (f) 0.00025 s

The relationship between fabric displacement and projectiles during the impact process is further explained through the phenomena visualized in Figure 9(a)-(e) on the observation time span. In Figure 9(a), when the projectile begins to penetrate the fabric, the displacement at S1 is lower than that of S0 and neat Kevlar. This is because friction between yarns holds the projectile from deforming the fabric. Smaller friction in neat Kevlar leads to greater deformation. The projectile continues to push the fabric in Figure 9(b), a pyramid-shaped deformation profile. In neat Kevlar, the fabric breaks because the strength of the thread exceeds the load by the ballistics. Kevlar with STF leaves yarns that hold projectiles with increasing amplitudes of deformation in fabrics globally. The higher the coefficient of friction, the greater the width of the pushed fabric [28], as shown by the dotted line in Figure 9(b) to (e). Neat Kevlar in all histories of penetration time, fabric width, and deformation amplitude has smaller values compared to S0 and S1. A greater coefficient of friction distributes the projectile load from the center toward the outlet and spreads indicated by the increase in the amplitude of fabric deformation [29].

Figure 10 shows the results of a comparison between simulations and experiments on fabric that has been impacted by a projectile. It seems that the final form of failure between simulation and experiment has similarities. On the net Kevlar, the final penetration shape is square, with a size of 6 x 6 mm. On the S0, the horizontal width of the penetrated scar is reduced to 5.5 mm, and the long horizontal length is extended to 7 mm. Then, on the S1, the penetrative scar has a larger shape than the other two fabrics, 6 x 9 mm. The similarities between the simulation and the experiment results indicate that the simulated model can describe the actual condition.

6. Stress

The tension on the fabric due to the projectile during the ballistic process is shown in Figure 10. Figure 11(a) shows the stress distribution at the beginning of the projectile pushing the fabric. The stress distribution on all three fabrics shows something similar. The stress at neat, S0, and S1 are 905, 904, and 811 MPa, respectively. The smaller the tension value of the fabric due to ballistic loads indicates the stronger the fabric because it can withstand greater impact forces without damage. At the time of $5x10^{-5}$ s (Figure 11(b)), the stress distribution changes. In neat Kevlar, the tension is evenly distributed throughout the fabric, while in Kevlar, to which STF is added, the tension is distributed along the axial axis of the fabric. S1 makes the deformation diameter larger than the other 2 types of fabric. Figure 11(c) shows the condition of the fabric at a time of $1x10^{-4}$ s. Stress distribution in neat Kevlar and S0 tends not to show changes like the previous conditions, while in S1 the stress distribution extends with the extent of the deformed area. At $1.5x10^{-4}$ s (Figure 11(d)), the fabric is lifted up so that the tension is lower than the previous condition. The stress on neat Kevlar is distributed at several points; the stress S0 is concentrated at the center of the fabric, and the stress S1 is distributed along the axial axis, followed by an increasingly large area of deformation. This state repeats itself until the end of time to $2.5x10^{-4}$ s (Figure 11(e)).

7. Fabric Failure Mechanism

The displacement and tension in the fabric due to ballistics have alluded to the stages of failure in the fabric. To further understand the effect of STF on failure, it is necessary to explain the mechanism of failure that occurs in fabrics in general. Fabric failure, according to [3],[30],[31], through 3 mechanisms, namely thickening, tearing, and fraction. Thickening is the phenomenon of changing the shape of the fabric at the impact site. Thickening occurs due to the transfer of kinetic energy of the projectile to the fabric [22]. Protrusions on the fabric can identify the presence of this phenomenon [30]. STF plays a significant role in the thickening of fabrics due to ballistics. Neat Kevlar deforms or forms a larger bulge height but with a smaller bulge area compared to S0 and S1. Larger bulge heights can cause yarns to break leading to tearing of the fabric due to too high deformation [32]. While a wider area of protrusion can have a positive impact on the fabric; namely, the kinetic energy of the projectile can be evenly distributed on the fabric [33]. The condition of the widespread area of protrusion due to ballistics is experienced by Kevlar fabric impregnated by STF. This is reinforced by the results of stress where S0 and S1 produce lower stress than neat Kevlar. STF that increases friction between yarns contributes to distributing ballistic loads throughout the fabric [34],[35]. Friction between yarns can prevent yarns from slipping on each other [34]. This is important to prevent the buildup of tension in a certain area that can cause the fabric to tear. Friction between yarns can help distribute kinetic energy from the projectile over a wider area by reducing local tension in the fabric [36]. STF also performs the same role in Kevlar fabrics that are subjected to tears and fragments. A tear occurs if the fabric is unable to withstand ballistic loads or, in theory, failure; the working load is greater than the strength of the material [37], [38]. Post-thickening, the fabric will continue to be pushed by the projectile until it breaks and breaks. In neat Kevlar, tears occur shorter due to higher thread deformation and local stress concentrated in the center of the fabric.

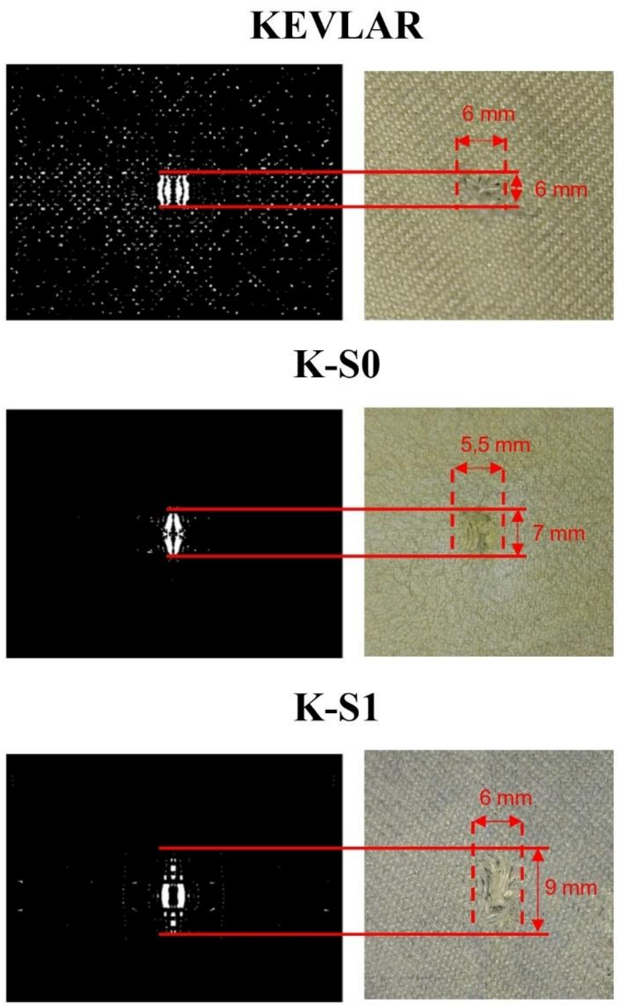

Fig.10. Comparison of simulation and experimental deformation results

Vol. 8, No. 1, July 2024, pp. 54-70

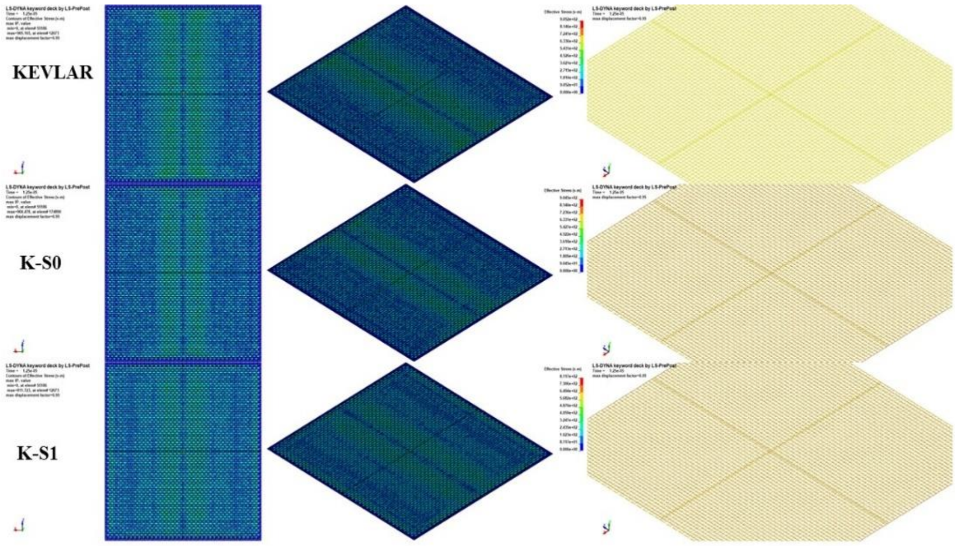

(a)

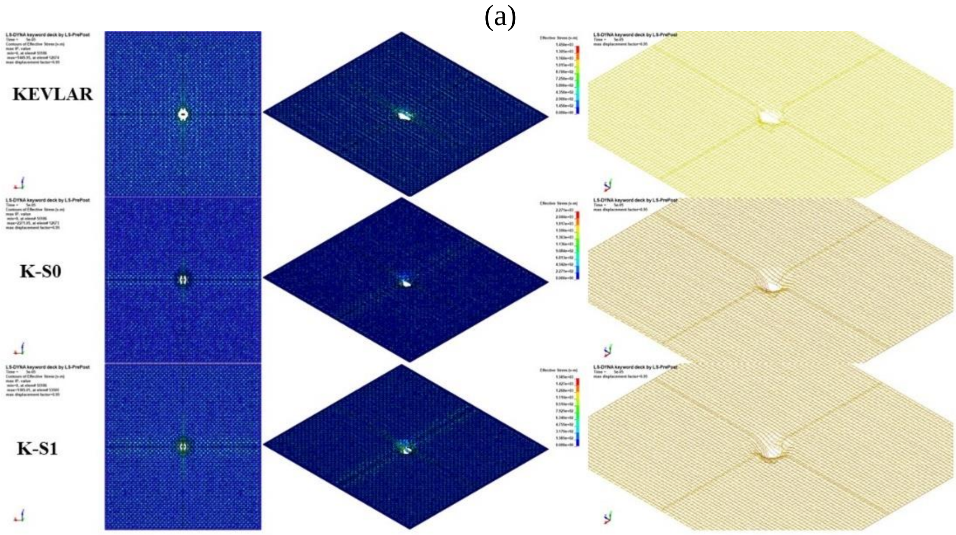

(b)

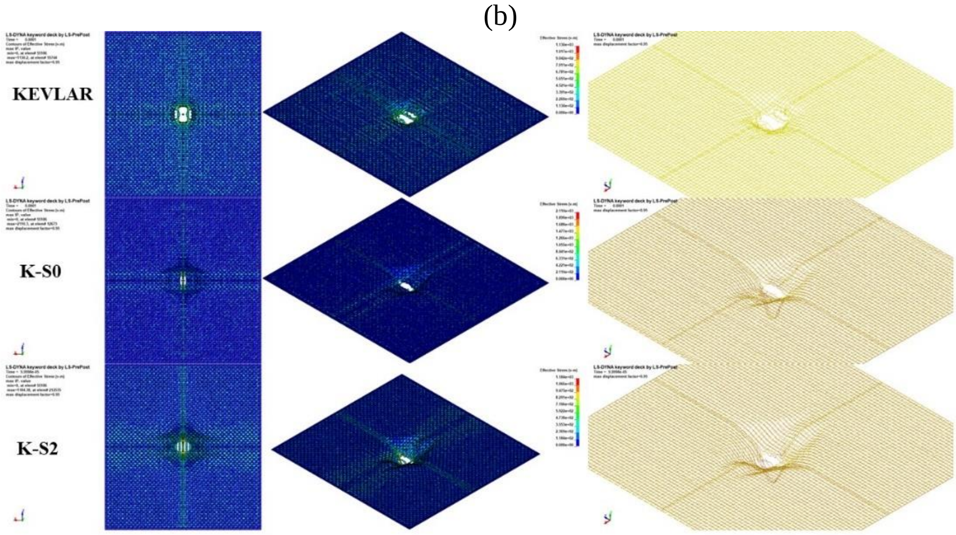

(c)

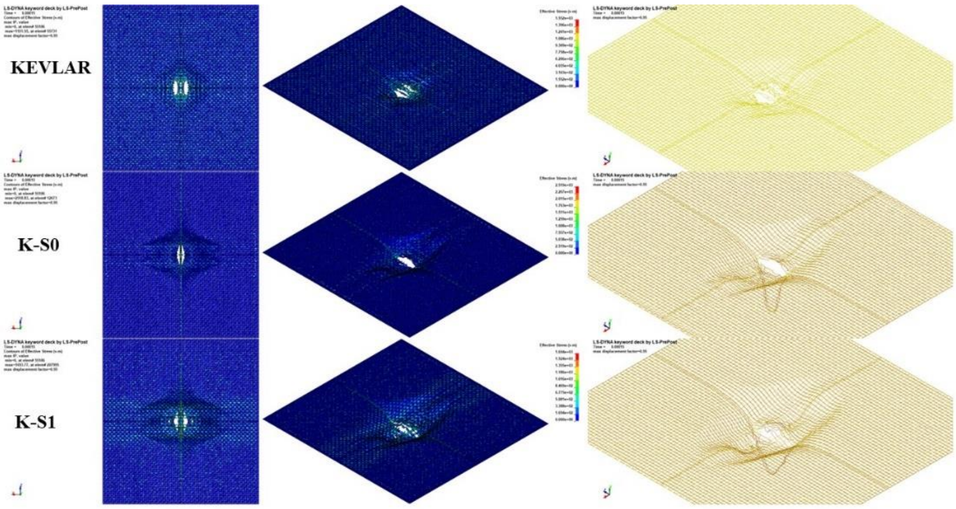

(d)

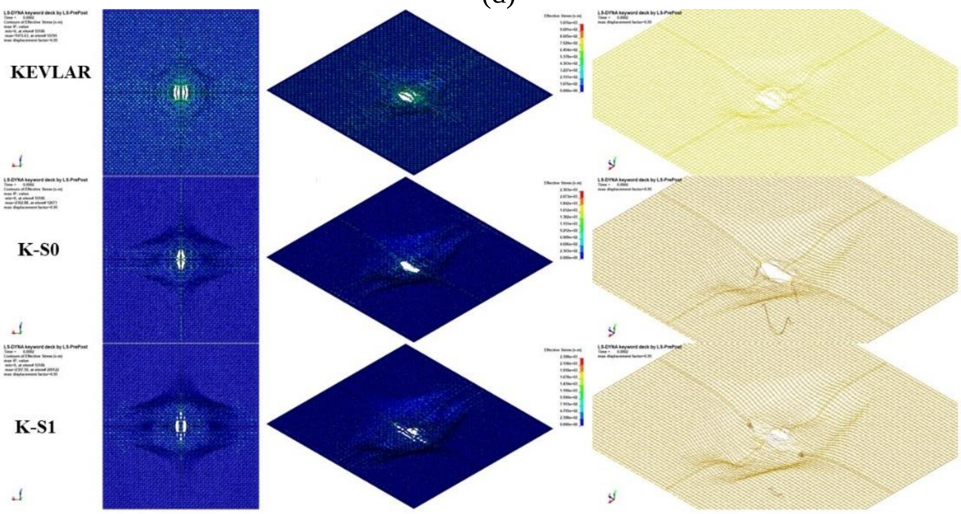

(e)

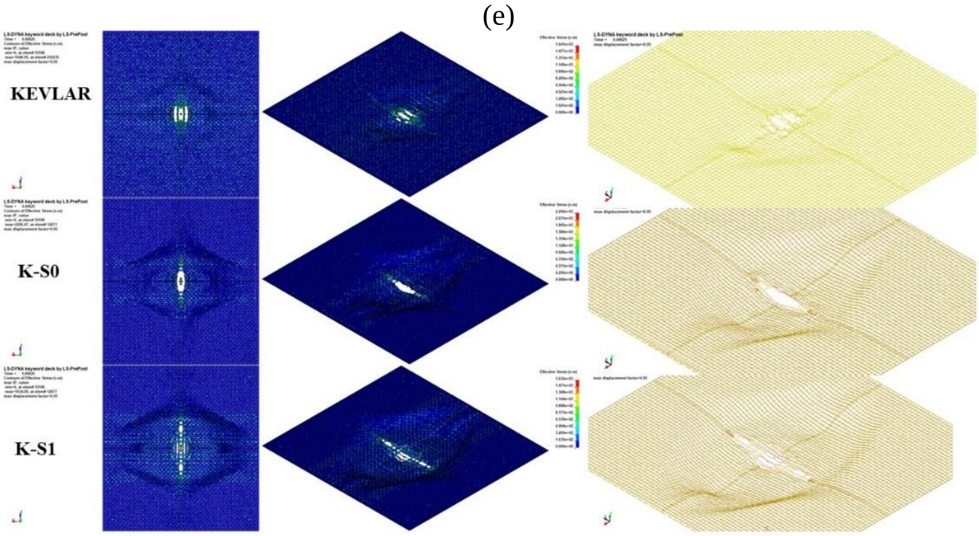

(f)

Fig. 11. Stress on fabric at time (a) 0.0000125; (b) 0.00005; (c) 0.0001; (d) 0.00015; (e) 0.0002; (f) 0.00025 s

IV. Conclusions

A simulation of the ballistic performance of STF-impregnated Kevlar was conducted, revealing significant enhancements in the fabric's protective capabilities. The variant impregnated with a second type of STF, specifically enriched with boron carbide (S1), exhibited superior performance due to an increase in the coefficient of friction between yarns, with static and dynamic coefficients measured at $\mu_s = 0.87$ and $\mu_d = 0.82$, respectively. This modification resulted in a notable reduction of the projectile's velocity to 153.2 m/s from an initial velocity of 200 m/s after penetrating the STF-impregnated fabric. Furthermore, the force exerted by the projectile on the S1 fabric escalated to 121,556 N, marking a threefold increase in comparison to unenhanced Kevlar. The application of STF significantly influenced the fabric's displacement and stress distribution upon ballistic impact, leading to greater displacement and more uniform stress distribution. The mechanism of failure, characterized by thickening, indicated that STF application effectively enlarges the fabric's deformation area upon impact. This disperses the ballistic kinetic energy more evenly across the fabric. Such enhancements align with the requirements for NIJ Level IIIA standards, suggesting that STF-impregnated Kevlar fabric, particularly the S1 variant, could offer a higher level of protection against high-velocity threats, thus potentially qualifying it as a viable material for NIJ Level IIIA ballistic protection applications.

Acknowledgment

This research was funded by PNBP UM Thesis Research scheme with contract number 5.4.775/UN32.20.1/LT/2023.

References

[1] S. Bocetta, "The History of Body Armor, From Medieval Times to Today | Small Wars Journal." Accessed: Apr. 29, 2023. [Online]. Available: https://smallwarsjournal.com/jrnl/art/the-history-of-body-armor-from-medieval-times-to-today

[2] U. Mawkhlieng and A. Majumdar, "Soft body armor," *Textile Progress*, vol. 51, No. 2, pp. 139–224, Apr. 2019, doi: 10.1080/00405167.2019.1692583.

[3] A. N. Nair, S. Sundharesan, and I. S. M. A. Tubi, "Kevlar-based composite material and its applications in body armor: A short literature review," *IOP Conf. Ser.: Mater. Sci. Eng.*, vol. 987, no. 1, p. 012003, Nov. 2020, doi: 10.1088/1757-899X/987/1/012003.

[4] I. G. Crouch, "Body armor – New materials, new systems," *Defence Technology*, vol. 15, no. 3, pp. 241–253, Jun. 2019, doi: 10.1016/j.dt.2019.02.002.

[5] S. Gürgen, W. Li, and M. C. Kuşhan, "The rheology of shear thickening fluids with various ceramic particle additives," *Materials & Design*, vol. 104, pp. 312–319, Aug. 2016, doi: 10.1016/j.matdes.2016.05.055.

[6] L. Wang, Z. Du, W. Fu, and P. Wang, "Study of mechanical property of shear thickening fluid (STF) for soft body-armor," *Mater. Res. Express*, vol. 8, no. 4, p. 045021, Apr. 2021, doi: 10.1088/2053-1591/abf76a.

[7] M. Zhao, J. Zhang, Z. Peng, and J. Zhang, "Effect of nano-solid particles on the mechanical properties of shear thickening fluid (STF) and STF-Kevlar composite fabric," *Journal of Engineered Fibers and Fabrics*, vol. 16, p. 155892502110448, Jan. 2021, doi: 10.1177/15589250211044817.

[8] L. Sun, G. Wang, C. Zhang, Q. Jin, and Y. Song, "On the rheological properties of multi-walled carbon nano-polyvinylpyrrolidone/silicon-based shear thickening fluid," *Nanotechnology Reviews*, vol. 10, no. 1, pp. 1339–1348, Sep. 2021, doi: 10.1515/ntrev-2021-0087.

[9] R. G. Egres and N. J. Wagner, "The rheology and microstructure of acicular precipitated calcium carbonate colloidal suspensions through the shear thickening transition," *Journal of Rheology*, vol. 49, no. 3, pp. 719–746, May 2005, doi: 10.1122/1.1895800.

[10] Q. He, S. Cao, Y. Wang, S. Xuan, P. Wang, and X. Gong, "Impact resistance of shear thickening fluid/Kevlar composite treated with shear-stiffening gel," *Composites Part A: Applied Science and Manufacturing*, vol. 106, pp. 82–90, Mar. 2018, doi: 10.1016/j.compositesa.2017.12.019.

[11] S. Cao, Q. Chen, Y. Wang, S. Xuan, W. Jiang, and X. Gong, "High strain-rate dynamic mechanical properties of Kevlar fabrics impregnated with shear thickening fluid," *Composites Part A: Applied Science and Manufacturing*, vol. 100, pp. 161–169, Sep. 2017, doi: 10.1016/j.compositesa.2017.04.015.

[12] K. Islam, M. A. Chowdhury, I. Hossain, and M. B. A. Shuvho, "Development and Characterization of kevlar-reinforced ceramic composite materials," *J. Test. Eval.*, vol. 49, no. 3, pp. 1631–1650, May 2021, doi: 10.1520/JTE20190873.

[13] R. Wei, B. Dong, W. Zhai, and H. Li, "Stab-resistant performance of the well-engineered soft body armor materials using shear thickening fluid," *Molecules*, vol. 27, no. 20, p. 6799, Oct. 2022, doi: 10.3390/moleculeS17206799.

[14] Y. Yang and X. Chen, "Determination of materials for hybrid design of 3D soft body armor panels," *Appl Compos Mater*, vol. 25, no. 4, pp. 861–875, Aug. 2018, doi: 10.1007/S00443-018-9716-y.

[15] M. A. Abtew, F. Boussu, and P. Bruniaux, "Dynamic impact protective body armor: A comprehensive appraisal on panel engineering design and its prospective materials," *Defence Technology*, vol. 17, no. 6, pp. 2027–2049, Dec. 2021, doi: 10.1016/j.dt.2021.03.016.

[16] Z. Xie, W. Chen, Y. Liu, L. Liu, Z. Zhao, and G. Luo, "Design of the ballistic performance of shear thickening fluid (STF) impregnated Kevlar fabric via numerical simulation," *Materials &; Design*, vol. 226, p. 111599, Feb. 2023, doi: 10.1016/j.matdes.2023.111599.

[17] X. Zhang, R. Yan, Q. Zhang, and L. Jia, "The numerical simulation of the mechanical failure behavior of shear thickening fluid/fiber composites: A review," *Polym Adv Technol*, vol. 33, No. 1, pp. 20–33, Jan. 2022, doi: 10.1002/pat.5512.

[18] S. Cao, H. Pang, C. Zhao, S. Xuan, and X. Gong, "The CNT/PSt-EA/Kevlar composite with excellent ballistic performance," *Composites Part B: Engineering*, vol. 185, p. 107793, Mar. 2020, doi: 10.1016/j.compositesb.2020.107793.

[19] S. Sen, N. B. Jamal M, A. Shaw, and A. Deb, "Numerical investigation of ballistic performance of shear thickening fluid (STF)-Kevlar composite," *International Journal of Mechanical Sciences*, vol. 164, p. 105174, Dec. 2019, doi: 10.1016/j.ijmecsci.2019.105174.

[20] J. C. Farias-Aguilar, M. J. Ramírez-Moreno, D. M. Gonzalez-García, L. Téllez-Jurado, and H. Balmori-Ramírez, "Evaluation of the ballistic protection level of (glass-fiber reinforced polyamide 6)-aramid fabric sandwich composite panels," *Journal of Materials Research and Technology*, vol. 12, pp. 1606–1614, May 2021, doi: 10.1016/j.jmrt.2021.03.088.

[21] Y. J. Xu, H. Zhang, and G. Y. Huang, "Ballistic performance of B4C/STF/Twaron composite fabric," *Composite Structures*, vol. 279, p. 114754, Jan. 2022, doi: 10.1016/j.compstruct.2021.114754.

[22] S. Gürgen, "Numerical modeling of fabrics treated with multi-phase shear thickening fluids under high velocity impacts," *Thin-Walled Structures*, vol. 148, p. 106573, Mar. 2020, doi: 10.1016/j.tws.2019.106573.

[23] X. Hong, Y. Ma, Z. Lei, R. Bai, H. Bai, X. Li, and J. Zou, "Analysis of interfacial friction properties of multi-phase STF/Kevlar composite fabrics in yarn pullout test," *Materials Today Communications*, vol. 34, p. 105086, Mar. 2023, doi: 10.1016/j.mtcomm.2022.105086.

[24] N. Asija, H. Chouhan, S. A. Gebremeskel, R. K. Singh, and N. Bhatnagar, "High strain rate behavior of STF-treated UHMWPE composites," *International Journal of Impact Engineering*, vol. 110, pp. 359–364, Dec. 2017, doi: 10.1016/j.ijimpeng.2017.02.019.

[25] A. M. Tarantino, L. Lanzoni, and F. O. Falope, "Numerical and experimental analyses," in *The Bending Theory of Fully Nonlinear Beams*, Cham: Springer International Publishing, 2019, pp. 49–70. DOI: 10.1007/978-3-030-14676-4_2.

[26] R. Bai, W. Li, Z. Lei, Y. Ma, F. Qin, Q. Fang, X. Chen, and Y. Chen, "Experimental study of yarn friction slip and fabric shear deformation in yarn pull-out test," *Composites Part A: Applied Science and Manufacturing*, vol. 107, pp. 529–535, Apr. 2018, doi: 10.1016/j.compositesa.2018.02.001.

[27] C. Du, F. Zeng, and B. Liu, "The Preparation of multifunctional shear thickening fluid and the application in shock absorber," *IOP Conf. Ser.: Earth Environ. Sci.*, vol. 639, no. 1, p. 012006, Jan. 2021, doi: 10.1088/1755-1315/639/1/012006.

[28] A. Khodadadi, G. Liaghat, S. Vahid, A. R. Sabet, and H. Hadavinia, "Ballistic performance of Kevlar fabric impregnated with nanosilica/PEG shear thickening fluid," *Composites Part B: Engineering*, vol. 162, pp. 643–652, Apr. 2019, doi: 10.1016/j.compositesb.2018.12.121.

[29] D. Dimeski, V. Srebrenkoska, and N. Mirceska, "Ballistic impact resistance mechanism of woven fabrics and their composites," *International Journal of Engineering Research*, vol. 4, no. 12, pp. 107-111, Dec. 2015.

[30] C. Ha-Minh, A. Imad, T. Kanit, and F. Boussu, "Numerical analysis of a ballistic impact on textile fabric," *International Journal of Mechanical Sciences*, vol. 69, pp. 32–39, Apr. 2013, doi: 10.1016/j.ijmecsci.2013.01.014.

[31] R. Wei, *W*. Zhai, X. Wang, W. Zhang, Y. Liang, B. Dong, and F. Li., "Preparation, characterization and properties of shear thickening fluid impregnated fabric composites," *IOP Conf. Ser.: Mater. Sci. Eng.*, vol. 423, no. 1, p. 012087, Oct. 2018, doi: 10.1088/1757-899X/423/1/012087.

[32] J. C. Farias-Aguilar, M. J. Ramírez-Moreno, D. M. Gonzalez-García, L. Téllez-Jurado, and H. Balmori-Ramírez, "Evaluation of the ballistic protection level of (glass-fiber reinforced polyamide 6)-aramid fabric sandwich composite panels," *Journal of Materials Research and Technology*, nol. 12, pp. 1606–1614, May 2021, doi: 10.1016/j.jmrt.2021.03.088.

[33] M. P. Ribeiro, P. H. P. M. da Silveira, F. de Oliveira Braga, and S. N. Monteiro, "Fabric impregnation with shear thickening fluid for ballistic armor polymer composites: An updated overview," *Polymers*, vol. 14, no. 20, Art. no. 20, Jan. 2022, doi: 10.3390/polym14204357.

[34] M. Bajya, A. Majumdar, and B. S. Butola, "Criticality of inter-yarn friction in high-performance fabrics for the design of soft body armor," *Composites Communications*, vol. 29, p. 100984, Jan. 2022, doi: 10.1016/j.coco.2021.100984.

[35] S. Ingle, C. S. Yerramalli, A. Guha, and S. Mishra, "Effect of material properties on ballistic energy absorption of woven fabrics subjected to different levels of inter-yarn friction," *Composite Structures*, vol. 266, p. 113824, Jun. 2021, doi: 10.1016/j.compstruct.2021.113824.

[36] S. Arora, A. Majumdar, and B. S. Butola, "Soft armor design by angular stacking of shear thickening fluid impregnated high-performance fabrics for quasi-isotropic ballistic response," *Composite Structures*, vol. 233, p. 111720, Feb. 2020, doi: 10.1016/j.compstruct.2019.111720.

[37] J. Lim, B. Lee, C. Lee, and I.-S. Han, "Effect of the weaving density of aramid fabrics on their resistance to ballistic impacts," *Engineering*, vol. 04, pp. 944–949, Jan. 2012, doi: 10.4236/eng.2012.412A119.

[38] A. Majumdar, A. Laha, D. Bhattacharjee, I. Biswas, and S. Verma, "Soft body armor development by silica particle based shear thickening fluid coated *p* -Aramid Fabrics," *The Journal of The Textile Institute*, vol. 110, no. 10, pp. 1515–1518, Oct. 2019, doi: 10.1080/00405000.2019.1602896.